Direct Greens function retrieval with internal multiples: an alternative to Marchenko focusing

Qiang Guo, Ivan Vasconcelos† and Tariq Alkhalifah**
**Physical Science and Engineering, King Abdullah University of Science & Technology (KAUST),*
†*Dept. of Earth Sciences, Utrecht University*

SUMMARY

Subsurface Green's functions provide crucial information for the seismic imaging and redatuming. A complete Green's functions containing the primary reflections and all orders of multiples can be utilized to mitigate artifacts and improve the resolution of seismic imaging. To fulfill this goal, some data-driven approaches using one-sided recorded data from the Earth's surface and a smooth migration velocity of the reference medium were developed. Among these approaches an iterative scheme was proposed using the multidimensional Marchenko equation based focusing functions. The iterative Marchenko approach is intrinsically designed to retrieve the coda of the focusing functions, which is supposed to handle all the internal multiples. The estimated focusing functions are then utilized to calculate the Green's functions by a crosscorrelation step. Inspired by the generalized internal multiple imaging (GIMI), we propose an approach that directly retrieves the Green's functions, instead of solving for the focusing functions. In the GIMI process, the reflection data are projected into the subsurface using the transmission information, followed by an interferometric step, which is similar to the multidimensional crosscorrelation of the Marchenko implementation. Thus, we derive a projected Marchenko equation from the relation between the Green's functions and the focusing functions, which reveals a clear connection to the GIMI. The new formulation offers an opportunity to solve for the Green's functions using an iterative scheme or by dealing with different orders of scattering, separately (a hierarchic approach). We introduce these two schemes and the corresponding adjoint operations, which enable us to adopt an optimization for data fitting. The basic performance of the two schemes are demonstrated on synthetic examples for the purpose of redatuming.

INTRODUCTION

Seismic imaging of the Earth's subsurface medium relies on Green's functions between the observation survey and the imaging points. The Green's functions of primary reflectivities can be easily retrieved from the recorded data using the provided migration velocity, which are commonly used in conventional imaging methods based on the single scattering assumption. The higher-order scattering that are embedded in the data as internal multiples end up showing as artifacts in the image, thus are often treated as noise (Berkhout and Verschuur, 1994). The internal multiples are generally with lower energy than the primary reflections, however, they play an important role in improving our ability to image complex structures, by providing additional illumination (Malcolm et al., 2009; Staal and Verschuur, 2013; Zuberi and Alkhalifah, 2014). An accurate estimation of the full Green's function produces a high-resolution image with less artifacts (Wapenaar et al., 2017), moreover, it provides the essential information to retrieve the subsurface localized wavefields that can be very useful for target-oriented inversion (Curtis and Halliday, 2010; Vasconcelos et al., 2017; Alkhalifah and Guo, 2018). Iterative substitution of the coupled Marchenko equations has been implemented to retrieve the Greens functions from a single-side acquisition surface to an arbitrary subsurface point (Behura et al., 2012; Wapenaar et al., 2014; van der Neut et al., 2015b). Focusing functions and causality-based windows are defined to solve the Marchenko equations. The preprocessed reflection response is substituted into the multidimensional crosscorrelation iteratively to solve for the focusing functions, which are then used to calculate the Green's functions. A direct approach to recognize the internal multiples is offered by the three-step GIMI process (Zuberi and Alkhalifah, 2014). It originally proposed to improve the imaging of complex subsurface structures that can be better illuminated by higher-order scattering. The second step of the GIMI process, which is an interferometric crosscorrelation with the reflection data, can be repeated to transform even higher orders of scattering into the leading order term for imaging. Alkhalifah and Guo (2018) showed that GIMI can be utilized to image different orders of multiples and they formulated a least-squares optimization to fit the multiple images to the corresponding data.

The GIMI approach can be applied to subsurface wavefield estimation through a separate optimization for different orders of multiple; besides that, it has similar operations to the Marchenko iterative solver as they both rely on concatenated multidimensional crosscorrelation. To find the relation between these two systems, we derive an approximate solution to retrieve the Green's functions directly from the Marchenko equation, which can be regarded as a projected version. This new equation, though not an exact inverse, shares the same form of implementation as GIMI, which simplifies the comparison. It weakens the role of the causality-based windows that is designed to estimate the intricate focusing functions in the Marchenko iterative approach. In this abstract, we propose two schemes to estimate the subsurface Green's functions based on the derived equation. Similar to the Marchenko approach, we can deploy an iterative scheme to retrieve the upgoing and downgoing Green's functions. Otherwise, benefitting from the knowledge we gained from GIMI, we can estimate the Green's functions related to different order scattering separately, we refer to as a hierarchic solution. The adjoint operation can then be formulated for the optimization of both schemes, which will help in producing cleaner virtual Green's functions. We also introduce a two-sided redatuming operation to retrieve the subsurface scattering wavefield based on the two schemes. More detailed results of the proposed least-squares optimization and the redatuming operations will be shared in the presentation of the work at the meeting.

A PROJECTED MARCHENKO EQUATION

We begin with the relation between the subsurface Green's functions and the focusing functions that is derived from the reciprocity theorem (Wapenaar et al., 2004):

$$\begin{bmatrix} -\mathbf{G}^{-} \\ \mathbf{G}^{+*} \end{bmatrix} = \begin{bmatrix} \mathbf{I} & -\mathbf{R} \\ -\mathbf{R}^{*} & \mathbf{I} \end{bmatrix} \begin{bmatrix} \mathbf{f}_1^{-} \\ \mathbf{f}_1^{+} \end{bmatrix}, \tag{1}$$

where the Green's functions $\mathbf{G}$ are related to the focusing functions $\mathbf{f}$ through a matrix composed of the reflection data $\mathbf{R}$. The superscript $^{-}$ and $^{+}$ indicate upgoing and downgoing wavefields, respectively. Instead of applying a causality-based window to solve the focusing functions, we aim to directly estimate the Green's function by multiplying a matrix

$$\mathbf{A} = \begin{bmatrix} \mathbf{I} & \mathbf{R} \\ \mathbf{R}^{*} & \mathbf{I} \end{bmatrix} \tag{2}$$

to both sides of the equation, which gives

$$\begin{bmatrix} \mathbf{I} & \mathbf{R} \\ \mathbf{R}^{*} & \mathbf{I} \end{bmatrix} \begin{bmatrix} -\mathbf{G}^{-} \\ \mathbf{G}^{+*} \end{bmatrix} = \begin{bmatrix} \mathbf{I}-\mathbf{R}\mathbf{R}^{*} & \mathbf{0} \\ \mathbf{0} & \mathbf{I}-\mathbf{R}^{*}\mathbf{R} \end{bmatrix} \begin{bmatrix} \mathbf{f}^{-} \\ \mathbf{f}^{+} \end{bmatrix}. \tag{3}$$

We move the matrix

$$\begin{bmatrix} \mathbf{I}-\mathbf{R}\mathbf{R}^{*} & \mathbf{0} \\ \mathbf{0} & \mathbf{I}-\mathbf{R}^{*}\mathbf{R} \end{bmatrix}$$

to the other side of equation 3 and multiply a windowing matrix of function Ψ, we get

$$\begin{bmatrix} \Psi & \mathbf{0} \\ \mathbf{0} & \Psi \end{bmatrix} \begin{bmatrix} \mathbf{I}-\mathbf{R}\mathbf{R}^{*} & \mathbf{0} \\ \mathbf{0} & \mathbf{I}-\mathbf{R}^{*}\mathbf{R} \end{bmatrix}^{-1} \mathbf{A} \begin{bmatrix} -\mathbf{G}^{-} \\ \mathbf{G}^{+*} \end{bmatrix} = \begin{bmatrix} \Psi & \mathbf{0} \\ \mathbf{0} & \Psi \end{bmatrix} \begin{bmatrix} \mathbf{f}^{-} \\ \mathbf{f}^{+} \end{bmatrix}. \tag{4}$$

The window function Ψ is designed to preserve the first arrival and the events after, thus gives $\Psi\mathbf{f}^{-} = \mathbf{0}$ and $\Psi\mathbf{f}^{+} = \mathbf{f}_{1,0}^{+}$, in which $\mathbf{f}_{1,0}^{+}$ represents the transmission component (van der Neut et al., 2015b). Based on the observation that the inverse matrix is diagonally dominant, we approximate it with an identity matrix, then we can rewrite equation 4 as

$$\begin{bmatrix} \Psi & \mathbf{0} \\ \mathbf{0} & \Psi \end{bmatrix} \begin{bmatrix} \mathbf{I} & \mathbf{R} \\ \mathbf{R}^{*} & \mathbf{I} \end{bmatrix} \begin{bmatrix} -\mathbf{G}^{-} \\ \mathbf{G}^{+*} \end{bmatrix} = \begin{bmatrix} \mathbf{0} \\ \mathbf{f}_{1,0}^{+} \end{bmatrix}, \tag{5}$$

where $\mathbf{f}_{1,0}^{+}$ can be computed using the migration velocity. We notice that equation 5 offers a direct estimation of the Green's functions without retrieving the focusing functions; meanwhile it does not require from us to deal with various combinations of window functions. The equation can be solved by calculating the least-squares inverse of the matrix $\mathbf{A}$, otherwise the Green's functions can be inverted using an iterative solver. A synthetic model with layered density (shown in Figure 1a) is used to analyze the performance of this projected equation.

The inverted upgoing and downgoing Green's functions are shown in Figure 2a, the summation of which provides a reasonably good match to the Green's function calculated using the true medium. For comparison, we show the inverted results using preconditioned Marchenko equation (van der Neut et al., 2015a) in Figure 2c. Figures 2b and 2d show the comparison for a trace, which indicates that the projected equation achieves reasonably accuracy, except with some small amplitude error compared to the inversion-based Marchenko solution.

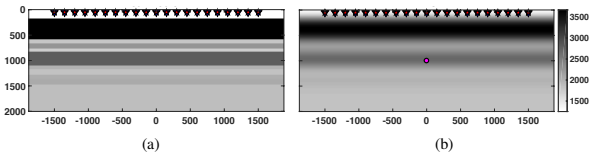

(a) (b)

Figure 1: The layered density model (a) with the acquisition geometry, (b) a smoothed version of the model and the datum point to evaluate the Green's function retrieval.

ITERATIVE AND HIERARCHIC SOLUTIONS

Though by solving the inverse of $\mathbf{A}$ we can obtain an approximate full Green's function estimation, in practive we rarely get the ideal data survey we need and the perfectly processed reflection response. On the other hand, we can take advantage of the iterative scheme to find an alternate optimization for the Green's function, which can be connected to the subsurface wavefield description based on GIMI. To retrieve the Green's functions by an iterative approach, we write equation 5 as

$$\begin{bmatrix} \Psi & \mathbf{0} \\ \mathbf{0} & \Psi \end{bmatrix} \begin{bmatrix} -\mathbf{G}^{-} + \mathbf{R}\mathbf{G}^{+*} \\ -\mathbf{R}^{*}\mathbf{G}^{-} + \mathbf{G}^{+*} \end{bmatrix} = \begin{bmatrix} \mathbf{0} \\ \mathbf{f}_{1,0}^{+} \end{bmatrix}. \tag{6}$$

The window function Ψ becomes trivial in the projected equation, as it simply preserves all the physical events. We thus mute Ψ in the following equations to abbreviate the expression. We have

$$\begin{cases} \mathbf{G}^{-} &= \mathbf{R}\mathbf{G}^{+*} \\ \mathbf{G}^{+*} &= \mathbf{R}^{*}\mathbf{G}^{-} + \mathbf{f}_{1,0}^{+} \end{cases}. \tag{7}$$

Initializing the downgoing Green's function by $\mathbf{f}_{1,0}^{+}$, we obtain for the first iteration

$$\begin{cases} \mathbf{G}_0^{+*} &= \mathbf{f}_{1,0}^{+} \\ \mathbf{G}_0^{-} &= \mathbf{R}\mathbf{G}_0^{+*} = \mathbf{R}\mathbf{f}_{1,0}^{+} \end{cases}, \tag{8}$$

which represents the first arrivals and primary reflections at the datum point, then we obtain the equations for the next two iterations as

$$\begin{cases} \mathbf{G}_1^{+*} &= \mathbf{f}_{1,0}^{+} + \mathbf{R}^{*}\mathbf{G}_0^{-} = \mathbf{f}_{1,0}^{+} + \mathbf{R}^{*}\mathbf{R}\mathbf{f}_{1,0}^{+} \\ \mathbf{G}_1^{-} &= \mathbf{R}\mathbf{G}_1^{+*} = \mathbf{R}\mathbf{f}_{1,0}^{+} + \mathbf{R}\mathbf{R}^{*}\mathbf{R}\mathbf{f}_{1,0}^{+} \end{cases}, \tag{9}$$

$$\begin{cases} \mathbf{G}_2^{+*} &= \mathbf{f}_{1,0}^{+} + \mathbf{R}^{*}\mathbf{R}\mathbf{f}_{1,0}^{+} + \mathbf{R}^{*}\mathbf{R}\mathbf{R}^{*}\mathbf{R}\mathbf{f}_{1,0}^{+} \\ \mathbf{G}_2^{-} &= \mathbf{R}\mathbf{f}_{1,0}^{+} + \mathbf{R}\mathbf{R}^{*}\mathbf{R}\mathbf{f}_{1,0}^{+} + \mathbf{R}\mathbf{R}^{*}\mathbf{R}\mathbf{R}^{*}\mathbf{R}\mathbf{f}_{1,0}^{+} \end{cases}, $$

and so on. These multidimensional crosscorrelation terms in the iterative solver correspond to the concatenated interferometry correlation of GIMI. Zuberi and Alkhalifah (2014) has proved, using the Born series, that repeating the multidimensional crosscorrelation to the reflection response actually transforms the energy of higher-order internal multiples to become the leading scattering term. Finally, the GIMI approach can image any order scattering, separately. Now, we have the iterative solver of equation 5, as well as the hierarchic solution to retrieve the Green's functions related to different orders of multiples

$$\begin{cases} \mathbf{G}_k^{m+*} &= (\mathbf{R}^{*}\mathbf{R})^{k}\mathbf{f}_{1,0}^{+} \\ \mathbf{G}_k^{m-} &= \mathbf{R}\mathbf{G}_k^{m+*} = \mathbf{R}(\mathbf{R}^{*}\mathbf{R})^{k}\mathbf{f}_{1,0}^{+} \end{cases}, \tag{10}$$

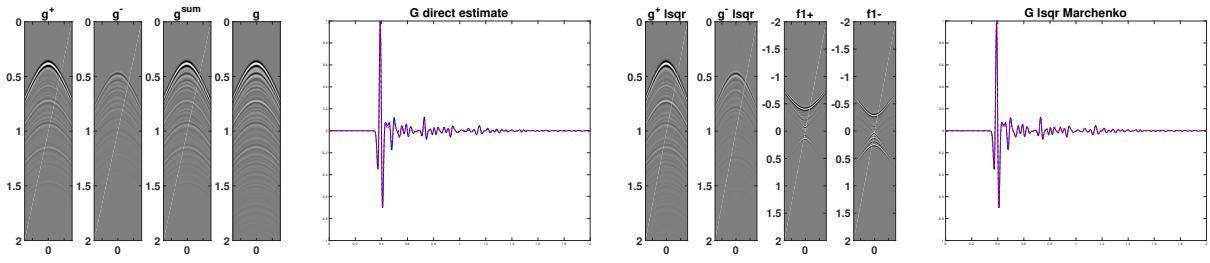

(a) (b) (c) (d)

Figure 2: The Green's functions retrieved by (a) the new projected equation and (c) the preconditioned inversion-based Marchenko; (b) and (d) are the comparison between the full Green's function and the estimated ones corresponding to (a) and (c). The full Green's function is shown in blue solid and the estimated is in red dash.

where the superscript ^{m} indicates the hierarchic solution. We apply the iterative and hierarchic solvers to the Marmousi model with variable density, shown in Figure 3. The recording is assumed on the surface, denoted by black stars (shots and receivers share the same geometry to satisfy the reciprocity requirement); the datum survey is in at depth 2.5 km. Figures 4a and 4b show the smoothed velocity used for the Green's function estimation and the window function Ψ computed from it. The upgoing and downgoing Green's functions calculated by the iterative approach at the first iteration are shown in Figure 5; the results of the second iteration are shown in Figure 6, followed by a summation, which we can then compare with the full Green's function in Figure 5. There are differences and some artifacts in the retrieved full Green's function, which we hope to mitigate in an optimization formulation.

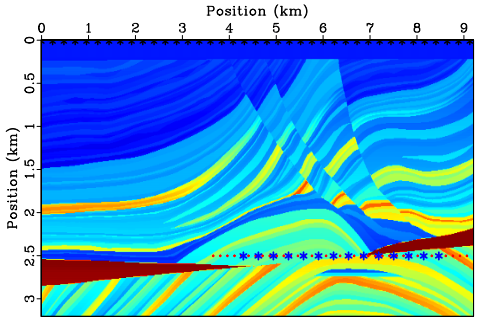

Figure 3: Marmousi velocity model with the acquisition geometry.

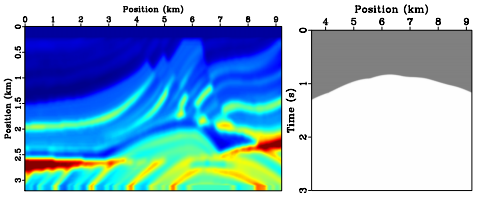

(a) (b)

Figure 4: The smoothed model (a) used to calculate (b) the window function Ψ.

THE ADJOINT OPERATIONS

Alkhalifah and Guo (2018) introduced the adjoint GIMI operation, based on the interferometric step, to generate the multiples from the corresponding high-order scattering images. Therefore, an optimization using a least-squares data fitting is developed to produce the separated images with higher resolution and less artifacts. The adjoint operation of the iterative solution used to fit the data is given by

$$\mathbf{R}_k = \mathbf{G}_k^+ \mathbf{G}_k^-, \tag{11}$$

which can be expanded in terms corresponding to different orders of scattering, e.g.

$$\begin{aligned}\mathbf{R}_2 &= \mathbf{G}_2^+\mathbf{G}_2^- = \mathbf{f}_{1,0}^{+*}\mathbf{R}\mathbf{f}_{1,0}^+ \\ &+ \mathbf{f}_{1,0}^{+*}\mathbf{R}^*\mathbf{R}\mathbf{R}\mathbf{f}_{1,0}^+ + \mathbf{f}_{1,0}^{+*}\mathbf{R}\mathbf{R}^*\mathbf{R}\mathbf{f}_{1,0}^+ + \mathbf{f}_{1,0}^{+*}\mathbf{R}^*\mathbf{R}\mathbf{R}^*\mathbf{R}\mathbf{f}_{1,0}^+,\end{aligned} \tag{12}$$

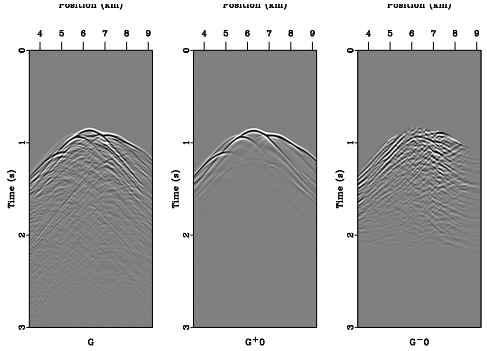

Figure 5: The full Green's function and the upgoing and downgoing Green's functions calculated by the iterative approach at the first iteration.

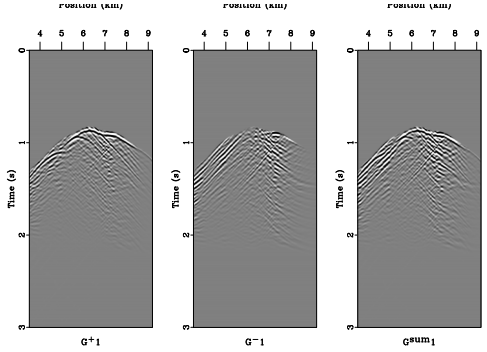

Figure 6: The upgoing and downgoing Green's functions calculated by the iterative approach at the second iteration and their summation, which is supposed to match the full Green's function.

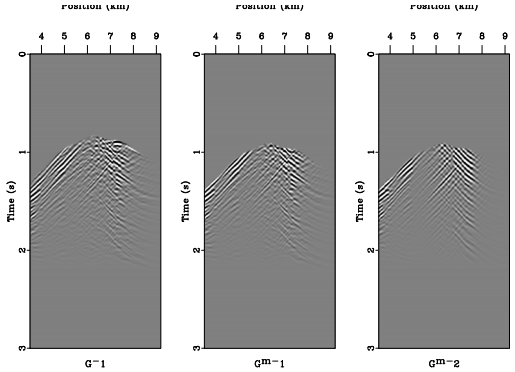

Figure 7: The downgoing Green's function calculated by the iterative approach, and the ones related to second- and third-order multiples by the hierarchic approach.

where $\mathbf{f}_{1,0}^{+*}\mathbf{R}\mathbf{f}_{1,0}^{+}$ reproduces the energy for single scattering, after that the secondary leading term $\mathbf{f}_{1,0}^{+*}\mathbf{R}^{*}\mathbf{R}\mathbf{R}\mathbf{f}_{1,0}^{+}$ corresponds to the interaction between the single scattering and the source of first-order multiple, which consists of double scattering, and then the last term induces higher-order scattering. Therefore, we have the adjoint operation that transform different orders of the subsurface Green's functions to the corresponding multiple reflection in the data:

$$\mathbf{R}_k^m = \mathbf{G}_0^{+}\mathbf{G}_k^{m-}, \tag{13}$$

which is consistent with the finding of Alkhalifah and Guo (2018). The adjoint operationcan be used to eliminate the crosstalk artifacts by deploying an least-squares optimization. Figure 7 shows the retrieved downgoing Green's functions containing the separated multiple scattering. Using the adjoint operations for the iterative scheme and the hierarchic solution, we reproduce the data representing the full scattering from below the datum and the one related to the second-order scattering, which are shown in Figure 8. The window function Ψ attenuates all the unphysical events from the overburden scattering.

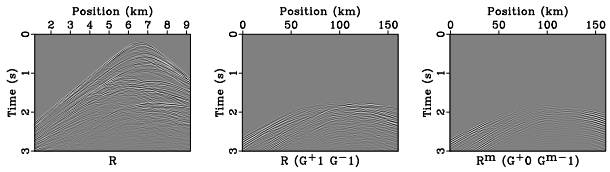

Figure 8: The observed reflection data, the modeled data using the adjoint for iterative full Green's function retrieval (after second iteration) and the adjoint for hierarchic approach of second-order scattering.

GENERALIZED REDATUMING USING INTERNAL MULTIPLES

Once we obtain the Green's function at the datum level, we can retrieve the scattering wavefield $\mathbf{D}$ of the underlying medium using (Vasconcelos et al., 2010)

$$\mathbf{D}_k(\mathbf{x},\mathbf{h}) = \mathbf{G}_k^{+*}(\mathbf{x})\mathbf{G}_k^{-}(\mathbf{x}+\mathbf{h}), \tag{14}$$

where $\mathbf{x}$ is the location vector of the virtual source and $\mathbf{h}$ is the subsurface offset (Hou and Symes, 2015). Similar to the GIMI process, we can also retrieve the virtual data from the separated multiples through

$$\mathbf{D}_k^m(\mathbf{x},\mathbf{h}) = \mathbf{G}_0^{+*}(\mathbf{x})\mathbf{G}_k^{m-}(\mathbf{x}+\mathbf{h}). \tag{15}$$

Accordingly, we formulate the adjoint operation for datuming using the iterative solution of the Green's functions as

$$\begin{aligned}\mathbf{R}_k &= \mathbf{G}_k^{-}(\mathbf{x})\mathbf{D}_k^{*}(\mathbf{x},\mathbf{h})\mathbf{G}_k^{+*}(\mathbf{x}+\mathbf{h})\mathbf{R}\\ &\text{or}\quad \mathbf{G}_k^{+}(\mathbf{x})\mathbf{D}_k(\mathbf{x},\mathbf{h})\mathbf{G}_k^{-*}(\mathbf{x}+\mathbf{h})\mathbf{R},\end{aligned} \tag{16}$$

and for the datuming using the Green's functions of separated multiples as

$$\begin{aligned}\mathbf{R}_k^m &= \mathbf{G}_k^{m-}(\mathbf{x})\mathbf{D}_k^{m*}(\mathbf{x},\mathbf{h})\mathbf{G}_0^{+*}(\mathbf{x}+\mathbf{h})\mathbf{R}\\ &\text{or}\quad \mathbf{G}_0^{+}(\mathbf{x})\mathbf{D}_k^{m}(\mathbf{x},\mathbf{h})\mathbf{G}_k^{m-*}(\mathbf{x}+\mathbf{h})\mathbf{R}.\end{aligned} \tag{17}$$

The virtual dataset at the datum calculated from the retrieved Green's functions after the second iteration is shown in Figure 9a, which show a reasonably good match with the data modeled from the true underlying medium.

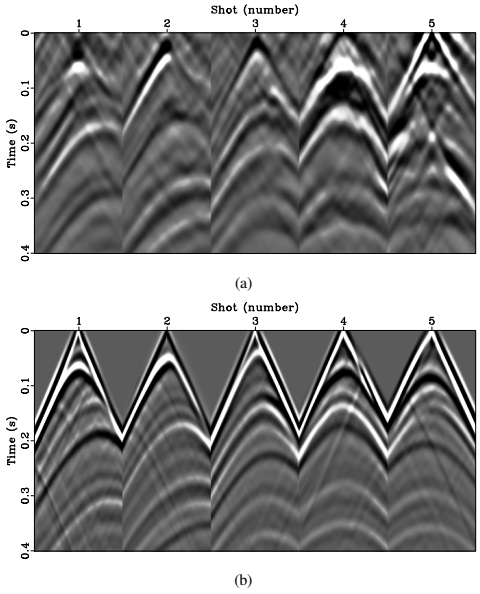

Figure 9: The retrieved subsurface scattering wavefield (a) and the modeled data at the datum (b) using the true underlying model.

DISCUSSIONS AND CONCLUSIONS

We first derived a projected Marchenko equation that can solve for subsurface Green's functions without calculating the focusing functions, and thus, reveals a clear connection to the GIMI approach. Both the Marchenko focusing equation and the projected equation can estimate the Green's functions by solving the inverse of the corresponding matrix. Inspired by the GIMI approach, we used the projected equation to devise iterative and hierarchic schemes of solutions. The adjoint operations for both schemes can then be formulated to fulfill a least-square data fitting optimization scheme. This optimization produced reasonable redatuming in the Marmousi model using a background smooth model.

REFERENCES

Alkhalifah, T., and Q. Guo, 2018, *in* Subsurface wavefields based on the generalized internal multiple imaging: 4337–4341.

Behura, J., K. Wapenaar, and R. Snieder, 2012, Newton-marchenko-rose imaging: , 1–6.

Berkhout, A. J., and D. J. Verschuur, 1994, *in* Part 2, migration of multiple reflections: 1497–1500.

Curtis, A., and D. Halliday, 2010, Source-receiver wave field interferometry: Phys. Rev. E, **81**, no. 4, 046601.

Hou, J., and W. W. Symes, 2015, An approximate inverse to the extended born modeling operator: GEOPHYSICS, **80**, R331–R349.

Malcolm, A. E., B. Ursin, and M. V. de Hoop, 2009, Seismic imaging and illumination with internal multiples: Geophysical Journal International, **176**, 847–864.

Staal, X., and D. Verschuur, 2013, Joint migration inversion, imaging including all multiples with automatic velocity update: 75th EAGE Conference & Exhibition incorporating SPE EUROPEC 2013.

van der Neut, J., J. Thorbecke, K. Wapenaar, and E. Slob, 2015a, Inversion of the multidimensional marchenko equation: Presented at the .

van der Neut, J., K. Wapenaar, and I. Vasconcelos, 2015b, On Green's function retrieval by iterative substitution of the coupled Marchenko equations: Geophysical Journal International, **203**, 792–813.

Vasconcelos, I., M. Ravasi, and J. van der Neut, 2017, Subsurface-domain, interferometric objective functions for target-oriented waveform inversion: GEOPHYSICS, **82**, A37–A41.

Vasconcelos, I., P. Sava, and H. Douma, 2010, Nonlinear extended images via image-domain interferometry: GEOPHYSICS, **75**, SA105–SA115.

Wapenaar, K., J. Thorbecke, and D. Draganov, 2004, Relations between reflection and transmission responses of three-dimensional inhomogeneous media: Geophysical Journal International, **156**, 179.

Wapenaar, K., J. Thorbecke, J. van der Neut, F. Broggini, E. Slob, and R. Snieder, 2014, Green's function retrieval from reflection data, in absence of a receiver at the virtual source position: The Journal of the Acoustical Society of America, **135**, 2847–2861.

Wapenaar, K., J. van der Neut, and E. Slob, 2017, Why multiples do not contribute to deconvolution imaging: Presented at the .

Zuberi, M. A. H., and T. Alkhalifah, 2014, Generalized internal multiple imaging (GIMI) using Feynman-like diagrams: Geophysical Journal International, **197**, 1582–1592.